Learning Phase Synchronization from Nonsynchronized Chaotic Regimes

Isao Tokuda,[1] Jürgen Kurths,[2] and Epaminondas Rosa, Jr.[3]
[1]Department of Computer Science and Systems Engineering, Muroran Institute of Technology, Muroran, Hokkaido 050-8585, Japan
[2]Nonlinear Dynamics, Institute of Physics, University of Potsdam, D-14415, Potsdam, Germany
[3]Department of Physics, Illinois State University, Normal, Illinois 61790
(Received 8 March 2001; published 17 December 2001)

We present a novel modeling approach for reconstruction of the global behavior of coupled chaotic systems from bivariate time series. We analyze two coupled chaotic oscillators, which are able to phase synchronize due to coupling. It is shown that our technique enables the recovery of the synchronization diagram from only three data sets. In particular, this allows the estimate of the relative strength of the coupling and the parameter mismatch of both subsystems. The method is most efficient if only data from the nonsynchronized regime are used for the model learning. We also apply this approach to experimental data of a paced plasma tube.

DOI: 10.1103/PhysRevLett.88.014101 PACS numbers: 05.45.Xt, 05.45.Tp, 52.35.Ra

The study of synchronization has a long history going back to Christiaan Huygens who observed synchronization of two pendulum clocks in 1673. This finding for periodic oscillators has been recently extended to chaotic systems, and four basic types of synchronization have been found: complete [1], generalized [2], phase [3], and lag synchronization [4]. Phase synchronization of coupled or periodically driven complex systems has found several applications (cf. Ref. [5], and references therein), including laboratory experiments, such as circuits [6], lasers [7], and plasmas [8], as well as natural systems, such as cardiorespiratory interaction [9,10], brain activity of Parkinsonian patients [11], paddlefish electrosensitive cells [12], Canadian lynx-hare populations [13], and solar activity [14].

To analyze such experimental data, some special techniques of synchronization analysis have been proposed and it has been shown that they are very efficient even for noisy and nonstationary data [5,9,11,15]. However, the important problem, how to reconstruct models from such synchronized data, remains open. It is of special interest to estimate the parameters that characterize the underlying coupled system such as the coupling strength of interaction between the two subsystems and the parameter mismatch of the two oscillators. These system parameters often cannot be measured, in particular in natural systems. To retrieve the synchronization regime of the underlying system, the reconstruction of a parametrized model family from sets of recording data is required.

There are several approaches to recover such a family from time series [16,17]. By using radial basis functions, the bifurcation diagram of a discrete-time dynamical system has been successfully reconstructed, however, under the restriction that the values of the bifurcation parameters that underlie each of the given time series are known *a priori* [18]. Also, a nonlinear regression technique based on maximal correlation enables one, in a nonparametric way, to retrieve the time delay in experimental laser data [19].

In the following, we focus on a special technique that enables us to estimate the underlying bifurcation parameters of dynamical systems [20]. By using nonlinear predictors, the algorithm reconstructs a bifurcation parameter family from a few sets of time series associated with different parameter values. This approach has the important practical advantage that no prior knowledge of the parametrized family of the dynamics, in particular the underlying bifurcation parameter values, is necessary. The efficiency of this technique has been shown for prototypical model systems of chaos, such as the Hénon, the Rössler, and the coupled delayed-logistic systems [20] and for nonstationary data [21].

Our purpose is to demonstrate this modeling approach applied to coupled or driven chaotic oscillators, using bivariate time series. The global behavior of the underlying system is learned from the observation of very few recorded data sets (no more than four), obtained from measurements made with different parameter values of the system.

We begin by describing our modeling technique. Suppose we have two coupled oscillators whose dynamical states are simultaneously recorded into bivariate time series $\{\xi_1(t), \xi_2(t)\}$. Among several dynamical components, only a single variable $\xi_{1,2}(t)$ is observed from each oscillator. With a change in the bifurcation parameters p, mainly the coupling strength and the parameter mismatch of both subsystems, the coupled system exhibits a variety of dynamical patterns, e.g., phase synchronization, nonphase synchronization, borderline between both, etc. We want to estimate the unknown parameter values $\{p_i\}_{i=1,\dots,N}$ associated with N sets of given bivariate time series $\{\xi_1(t, p_i), \xi_2(t, p_i)\}_{i=1,\dots,N}$ under the conditions that (A) the time series are obtained from nonphase synchronized chaotic regimes and (B) all data come from the same attractor whose qualitative structure is changed by the bifurcation parameters.

The main idea of our approach is to compute Γ which are qualitatively similar to the original parameters p. For

 0031-9007/02/88(1)/014101(4)$15.00

a one-to-one correspondence between Γ and p, Γ gives rise to a parametrized family of nonlinear dynamics $F(\Gamma, \cdot)$ which exhibits qualitatively similar bifurcation phenomena inherent to the original system.

Our algorithm is mainly composed of two steps (the detailed algorithm will be described in full in a future paper).

(i) Embed the bivariate time series $\{\xi_1(t), \xi_2(t)\}$ into delay coordinates [22]: $X_1 = \{\xi_1(t), \xi_1(t-\tau), \ldots, \xi_1(t-(d-1)\tau)\}$, $X_2 = \{\xi_2(t), \xi_2(t-\tau), \ldots, \xi_2(t-(d-1)\tau)\}$. Construct, within the same parametrized family, two coupled nonlinear predictors $F_{1,2}$ that model the N sets of time series as

$$\frac{dX_1}{dt} = F_1(W, X_1, X_2),$$
$$\frac{dX_2}{dt} = F_2(W, X_2, X_1). \tag{1}$$

This means that we seek the N sets of nonlinear prediction parameters $\{W(p_i)\}_{i=1,\ldots,N}$ that correspond to each time series $\{\xi_1(t, p_i), \xi_2(t, p_i)\}_{i=1,\ldots,N}$ (learning algorithm of the nonlinear predictors is described in detail in Ref. [20]). Note that the dimension of the prediction parameters W is larger than that of the original parameters p. For the nonlinear predictors $F_{1,2}$, any global functional model, such as polynomial functions [17] or radial basis functions [18], may be used. In this paper, we exploit a three-layer feed-forward neural network [23] having $2d$ units in the input layer and d units in the output layer for each $F_{1,2}$.

(ii) Use the singular value decomposition to extract the principal components Γ from the nonlinear prediction parameters $\{W(p_i)\}_{i=1,\ldots,N}$. The number of the principal components Γ is determined in such a way that the sum of the normalized eigenvalues that measure significances of the principal components is larger than 0.95. On this principal component parameter space Γ, we define a parametrized family of coupled nonlinear predictors $F_{1,2}$. By computing the mean frequency difference of the nonlinear predictors $F_{1,2}$, which depends upon the principal component parameter values Γ, the synchronization diagram, i.e., the region of phase synchronization and its borderline, is recovered.

The present algorithm is based on the following mechanism. Suppose that a coupled nonlinear system $f_{1,2}(p)$ whose bifurcation parameters are fixed as $p = p^*$ is modeled by $F_{1,2}(W^*)$. When the original parameters p^* are slightly perturbed as $p^* + \Delta p$, we can expect from the smoothness of nonlinear dynamics that the corresponding model is given by $F_{1,2}(W^* + \Delta W)$, which is also a slight perturbation of the model parameters W^*. In this way, in parameter space around p^* and W^*, there may exist a one-to-one correspondence between the original and the model parameters. The original parameter space p which is projected into the model parameter space W is extracted via the singular value decomposition.

Next we apply this technique to two bidirectionally coupled Rössler oscillators [3], $\dot{x}_{1,2} = -\omega_{1,2}y_{1,2} - z_{1,2} + C(x_{2,1} - x_{1,2})$, $\dot{y}_{1,2} = \omega_{1,2}x_{1,2} + 0.15y_{1,2}$, $\dot{z}_{1,2} = 0.2 + z_{1,2}(x_{1,2} - 10)$. We analyze the case where the subsystems are not identical, but have a mismatch $\Delta\omega$ in the parameters $\omega_{1,2} = 1 \pm \Delta\omega$. A systematic dependence of the synchronization region on the coupling strength C and the parameter mismatch $\Delta\omega$ is shown in Fig. 1. To learn the global behavior of this coupled system with dependence on both parameters, we simulate data records for only three different parameter arrangements. For three sets of different parameter values, $(C, \Delta\omega) = (0.06, 0.045)$, $(0.05, 0.04)$, $(0.06, 0.035)$ (Fig. 1), the corresponding bivariate time series $\{\xi_1(t), \xi_2(t)\}_{i=1,2,3}$ are recorded for a time interval of 100 with a sampling rate of 0.05. For the time series variables $\xi_{1,2}$, we pick the $y_{1,2}$ coordinate from each oscillator.

At the first step of the algorithm, the time lag and the embedding dimension are set as $(\tau, d) = (0.2, 3)$. Next, we model each of the three records using the coupled nonlinear predictors [Eqs. (1)]. By singular value decomposition, two-dimensional principal component parameters (Γ_1, Γ_2) are extracted from the three sets of 160 nonlinear prediction parameters corresponding to the three records. We then perform a linear rescaling of this space, in order to bring these parameters into close correspondence with the system's parameters C and $\Delta\omega$. Without any knowledge of the dynamical system, it is, in principle, impossible to find correspondence between the system's parameters and the principal components. Nevertheless, since we are interested in a particular parameter, i.e., the coupling strength parameter, its corresponding parameter can be identified. We rewrite the principal components in polar coordinates $(\Gamma_1, \Gamma_2) = (r\cos\theta, r\sin\theta)$ and determine the optimal angle θ_{opt} that corresponds to coupling strength C. The main point of this optimization is to find the θ value that has the strongest influence on the coupling parameters $\{W_k: k \in \text{coupling}\}$ of the nonlinear predictors $F_{1,2}$. This subset of the prediction parameters includes all those

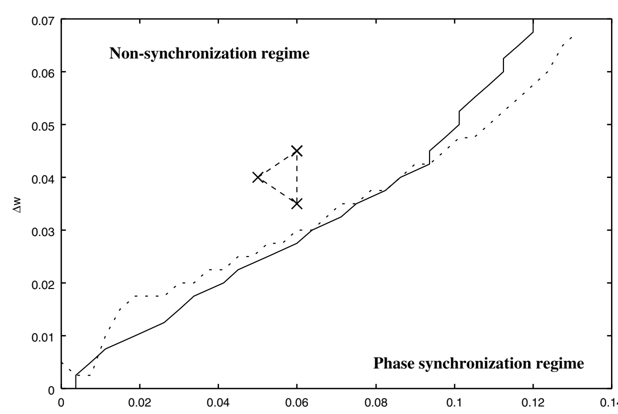

FIG. 1. Borderlines between regimes of phase synchronization and nonsynchronization for the two coupled Rössler oscillators (solid line) and the coupled nonlinear predictors (dotted line). The triangle indicates the locations of the three sets of parameter values used for the learning of the neural networks.

which couple X_1 and X_2 in Eqs. (1). Their influence is measured by the mean variance $\delta W(\theta)$ of the coupling parameters for a variation of radii $\{r = i/40: i = -40, -39, \ldots, 40\}$. The mean variance δW is then normalized by using 500 sets of the mean variances computed for randomly selected parameters of the nonlinear predictors. From this bootstrapping technique, we calculate Theiler *et al.*'s [24] significance value $S(\theta)$ and get a maximum for $\theta_{\rm opt} = 0.251$, which gives $S = 5.34$, a good level of significance. The significance test, therefore, infers correspondence between the original parameters and the principal components as $C \leftrightarrow \Gamma_1 \cos\theta_{\rm opt} - \Gamma_2 \sin\theta_{\rm opt}$ and $\Delta\omega \leftrightarrow \Gamma_1 \sin\theta_{\rm opt} - \Gamma_2 \cos\theta_{\rm opt}$. The synchronization diagram of the coupled nonlinear model [Eqs. (1)] is finally drawn on this corresponding principal component space. The model diagram of Fig. 1 shows a surprising similarity to the original one.

It is important to note that the most efficient way to reconstruct the synchronization diagram is to use only the data from nonphase synchronization regimes as in the above experiment. In the phase synchronization regimes, there exists a low-dimensional nonlinear manifold in which the phase synchronization dynamics is constrained. If we use only the data from the phase synchronization regimes, prediction of the nonsynchronized dynamics seems to be very hard because such data do not contain any dynamical information from outside of the phase synchronization manifold.

As the second example, a periodically forced Rössler system, $\dot{x} = -y - z + E\cos\Omega t$, $\dot{y} = x + 0.15y$, $\dot{z} = 0.4 + z(x - 8.5)$, is analyzed [25]. For the modeling of this driven system, an input-output model $\frac{d}{dt}X_1 = F_1(W, X_1, X_2)$ is used instead of the coupled model [Eqs. (1)]. By assuming that the driving force signal is recorded as the second component of the bivariate time series as $\xi_2(t) = \cos\Omega t$, we model only the forced system F_1 which has $X_2 = \{\cos\Omega t, \cos(\Omega t - \tau), \ldots, \cos(\Omega t - (d-1)\tau)\}$ as the input signals. Because of this simpler task, we take only two different parameter values for input intensity as $E = 0, 0.5$ and obtain the corresponding bivariate time series $\{y(t), \cos\Omega t\}$ for a time interval of 20π with a sampling rate of $\pi/64$. The driving frequency is fixed as $\Omega = 1.04$. We model the two records using the input-output model with $(\tau, d) = (0.2, 3)$ and extract a single principal component parameter Γ_1 by singular value decomposition of 80 model parameters. With dependence on the driving frequency Ω and the principal component parameter Γ_1, which is scaled to match the corresponding intensity parameter E of the original system, the borderline between the synchronized and nonsynchronized regimes of the input-output model is again in good agreement with the original (Fig. 2).

We now test whether our technique also works for experimental data. We analyze experimental data from a chaotic plasma discharge tube subject to the action of a periodic wave generator, a paradigmatic experiment for chaos phase synchronization [8]. This tube (Geissler tube) is filled with spectroscopically pure helium gas, and the anode and cathode are connected to a high dc voltage (850 V) through a current limiting resistor $R = 30$ kΩ. In parallel with the resistor, a capacitor $C = 3.5$ pF cuts out the high voltage, and a transformer adds a very low amplitude sine wave (range 0–0.4 V) pacing the whole system.

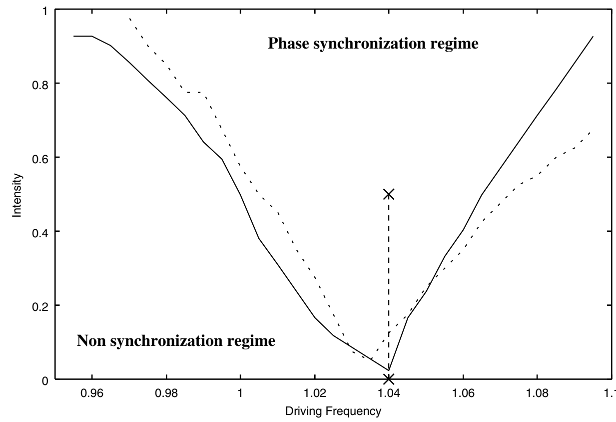

FIG. 2. Borderlines between regimes of phase synchronization and nonsynchronization for the forced Rössler system (solid line) and the input-output model (dotted line). The two crosses indicate the locations of the two sets of parameter values used for the learning of the neural networks.

Because this is similar to the periodically forced Rössler system, we again try to learn the global behavior from data with only two different pacing parameters. As an experimental measurement $\xi(t)$, the current through the plasma is used, where one record is non-paced and the other is paced with a pacing frequency of 6960 Hz and an amplitude of 0.4 V. The paced data is in a phase synchronized regime and the sampling rate is set as 200 kHz. Similarly to our analysis of the driven Rössler model above, a synchronization diagram of the plasma system is reconstructed by using two sets of bivariate time series $\{\xi(t), \cos\Omega t\}$ with $\Omega = 2\pi * 6960$. We model the two records using the input-output model with $(\tau, d) = (7/200000, 3)$ and extracted a single principal component parameter Γ_1 by singular value decomposition of 100 model parameters. By changing the pacing frequency Ω and the principal component parameter Γ_1, which is scaled to match the real pacing amplitude, the borderline between the regimes of phase synchronization and nonphase synchronization is drawn with the dotted line in Fig. 3. This is an Arnold tongue-like shape similar to the original borderline (solid line of Fig. 3) obtained directly from experimental data [8]. In this case locations of the two borderlines do not show the same level of agreement as before because (a) experimental results are subject to all sorts of distortion and noise and (b) one set of data used is from a synchronization regime.

To conclude, the modeling approach presented in this Letter enables us to reconstruct the synchronization diagram of coupled or forced chaotic oscillators from a few records of bivariate time series. Our technique allows us

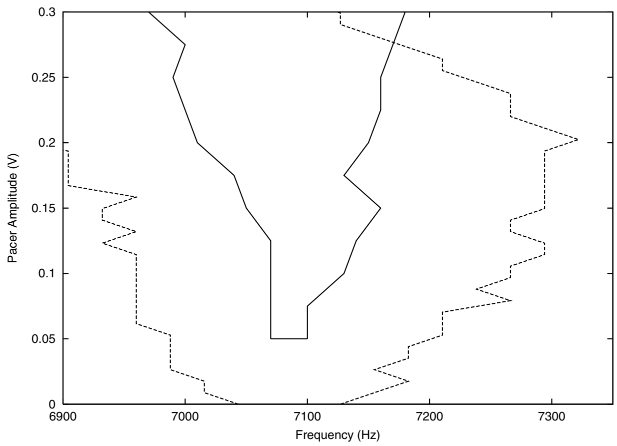

FIG. 3. Borderlines between regimes of phase synchronization and nonsynchronization for a paced chaotic plasma discharge (solid line) and the input-output model (dotted line). The plasma data is recorded from the real experiment of Ref. [8].

to estimate the relative strength of coupling and to evaluate how close a system is to the borderline of phase synchronization and nonphase synchronization in experimental systems, even when no further information about the underlying dynamics is available. This should be of importance especially for natural coupled system [5], e.g., in neural systems, parasystole, circadian rhythms, insulin dynamics, vocal fold vibrations, locomotion, and ventilation versus respiration.

Practical application of the present technique might be limited in case (*a*) recording data are contaminated with strong observational or dynamical noise or (*b*) the dynamical system has strong nonlinearity or discontinuity. Our future studies will deal with these problems and will also apply the present technique to coupled stochastic nonlinear systems and a network of many coupled oscillators.

[1] L. M. Pecora and T. L. Carroll, Phys. Rev. Lett. **80**, 2109 (1990).

[2] N. F. Rulkov, M. M. Sushchik, L. S. Tsimring, and H. D. I. Abarbanel, Phys. Rev. E **51**, 980 (1995); L. Kocarev and U. Parlitz, Phys. Rev. Lett. **76**, 1816 (1996); K. Josic, Phys. Rev. Lett. **80**, 3053 (1998).

[3] M. G. Rosenblum, A. S. Pikovsky, and J. Kurths, Phys. Rev. Lett. **76**, 1804 (1996).

[4] M. G. Rosenblum, A. S. Pikovsky, and J. Kurths, Phys. Rev. Lett. **78**, 4193 (1997).

[5] Special issue, *Phase Synchronization and its Applications,* edited by J. Kurths, Int. J. Bifurcation Chaos Appl. Sci. Eng. **10–11** (2000); A. Pikovsky, M. Rosenblum, and J. Kurths, *Synchronization—A Universal Concept in Nonlinear Sciences* (Cambridge University Press, Cambridge, UK, 2001).

[6] U. Parlitz, L. Junge, W. Lauterborn, and L. Kocarev, Phys. Rev. E **54**, 2115 (1996); S. Taherion and Y.-C. Lai, Int. J. Bifurcation Chaos Appl. Sci. Eng. **11**, 2587 (2000).

[7] E. Lariontsev, Int. J. Bifurcation Chaos Appl. Sci. Eng. **10**, 2441 (2000); E. Allaria, F. T. Arecchi, A. DiGarbo, and R. Meucci, Phys. Rev. Lett. **86**, 787 (2001).

[8] C. M. Ticos, E. Rosa, Jr., W. B. Pardo, J. A. Walkenstein, and M. Monti, Phys. Rev. Lett. **85**, 2929 (2000); E. Rosa *et al.,* Int. J. Bifurcation Chaos Appl. Sci. Eng. **10**, 2551 (2000).

[9] C. Schafer, M. G. Rosenblum, J. Kurths, and H.-H. Abel, Nature (London) **392**, 239 (1998).

[10] V. S. Anishchenko *et al.,* Int. J. Bifurcation Chaos Appl. Sci. Eng. **10**, 2339 (2000); A. Stefanovska *et al.,* Phys. Rev. Lett. **85**, 4831 (2000).

[11] P. Tass *et al.,* Phys. Rev. Lett. **81**, 3291 (1998).

[12] A. Neiman *et al.,* Phys. Rev. Lett. **82**, 660 (1999); A. Neiman *et al.,* Int. J. Bifurcation Chaos Appl. Sci. Eng. **10**, 2499 (2000).

[13] B. Blasius, A. Huppert, and L. Stone, Nature (London) **399**, 354 (1999); B. Blasius and L. Stone, Int. J. Bifurcation Chaos Appl. Sci. Eng. **10**, 2361 (2000).

[14] M. Palus, J. Kurths, U. Schwarz, D. Novotna, and I. Charvatova, Int. J. Bifurcation Chaos Appl. Sci. Eng. **10**, 2519 (2000).

[15] N. B. Janson, A. G. Balanov, V. S. Anishchenko, and P. V. E. McClintock, Phys. Rev. Lett. **86**, 1749 (2001).

[16] H. D. I. Abarbanel, *Analysis of Observed Chaotic Data* (Springer-Verlag, New York, 1996); H. Kantz and T. Schreiber, *Nonlinear Time Series Analysis* (Cambridge University Press, Cambridge, 1997).

[17] J. P. Crutchfield and B. S. McNamara, Complex Systems **1**, 417 (1987).

[18] M. Casdagli, Physica (Amsterdam) **35D**, 335 (1989).

[19] H. Voss and J. Kurths, Phys. Lett. A **234**, 336 (1997).

[20] R. Tokunaga, S. Kajiwara, and T. Matsumoto, Physica (Amsterdam) **79D**, 348 (1994); I. Tokuda, S. Kajiwara, R. Tokunaga, and T. Matsumoto, Physica (Amsterdam) **95D**, 380 (1996).

[21] I. Tokuda, R. Tokunaga, and T. Matsumoto, Physica (Amsterdam) **135D**, 63 (2000).

[22] F. Takens, in *Dynamical Systems and Turbulence,* edited by D. A. Range and L. S. Young, Lecture Notes in Mathematics (Springer, Berlin, 1981), Vol. 898, p. 366; T. Sauer, J. A. York, and M. Casdagli, J. Stat. Phys. **65**, 579 (1991).

[23] G. Cybenko, Math. Control Signals Syst. **2**, 303 (1989); K. Funahashi, Neural Netw. **2**, 183 (1989); K. Hornik, Neural Netw. **2**, 359 (1989).

[24] J. Theiler, S. Eubank, A. Longtin, B. Galdrikian, and J. D. Farmer, Physica (Amsterdam) **58D**, 77 (1992); J. Theiler and D. Prichard, Physica (Amsterdam) **94D**, 221 (1996).

[25] A. S. Pikovsky, M. G. Rosenblum, G. Osipov, and J. Kurths, Physica (Amsterdam) **104D**, 219 (1997).